Fish and Shellfish Immunology 86 (2019) 981–993

Contents lists available at ScienceDirect

Fish and Shellfish Immunology

journal homepage: www.elsevier.com/locate/fsi

Full length article

Molecular cloning and expression analysis of C-type lectin (RpCTL) in Manila clam *Ruditapes philippinarum* after lipopolysaccharide challenge

Dongdong Li[a,b], Hongtao Nie[a,b,*], Shasha Dong[a,b], Zhongming Huo[a,b], Xiwu Yan[a,b,**]

[a] Engineering and Technology Research Center of Shellfish Breeding in Liaoning Province, Dalian Ocean University, Dalian, 116023, China
[b] College of Fisheries and Life Science, Dalian Ocean University, Dalian, 116023, China

ARTICLE INFO

Keywords:
Ruditapes philippinarum
C-type lectin
Immune defense
Expression profile
Pattern recognition receptor

ABSTRACT

The Manila clam, *Ruditapes philippinarum*, is one of the most commercially important marine bivalves. C-type lectins (CTLs) are pattern recognition receptors (PRRs) that play important roles in the identification and elimination of pathogens by the innate immune system. In this study, a new CTL (RpCTL) was identified in the Manila clam, *R. philippinarum*. The full-length RpCTL cDNA is 802 bp, with an open reading frame of 591 bp, encoding 196 amino acids, including an N-terminal signal peptide and a carbohydrate recognition domain (CRD). RpCTL contains conserved CRD disulfide bonds involving four cysteine residues (Cys^{30}–Cys^{104}, Cys^{124}, and Cys^{132}), and the EPN (Glu^{94}–Pro^{95}–Asn^{96}) and WND (Trp^{119}–Asn^{120}–Asp^{121}) motifs. Quantitative reverse transcription (RT)–PCR detected *RpCTL* transcripts mainly in the gill, siphon, and hepatopancreas in three shell-color strains (zebra, white, and white–zebra strains) and two unselected populations of *R. philippinarum*, and the gene was highly expressed in the hepatopancreas after lipopolysaccharide treatment. Antimicrobial activity assays of recombinant RpCTL against both Gram-positive and Gram-negative bacteria showed that RpCTL inhibits microorganismal growth. In a survival test, RpCTL inhibited and killed *Vibrio anguillarum* in *R. philippinarum*. These results suggest that RpCTL participates in the pathogen identification process of *R. philippinarum* as a PRR and in its immune defense system.

1. Introduction

The innate immune system is the first line of defense against foreign substances and pathogenic microorganisms, and is considered to be the primitive and general form of host defenses [1]. Most invertebrates lack acquired immunity because these animals do not express memory immunoglobulins after the first pathogen attack [2]. Higher vertebrates, such as birds and mammals, have adaptive immune defense responses, whereas fish and amphibians are largely dependent on the innate immune system [3]. In recent years, research into the C-type lectins (CTLs) has been reported in various invertebrates, including insects, mollusks, and crustaceans [4–7], and a number of studies in marine bivalve species have also been published, including in the clam [8], abalone [9], oysters [10], and scallops [11]. Symbiotic and pathogenic bacteria are identified by CTLs in the white calm *Codakia orbicularis*. C-type lectins are significantly induced in the Zhikong scallop *Chlamys farreri* by *Vibrio anguillarum*, and a recombinant protein showed agglutination activity against different microorganisms [12–14]. The recognition process is mediated by highly conserved pattern recognition receptors (PRRs), which are components of the innate immune system in invertebrates [15,16]. Each PRR can identify a set of microbial components with similar structural patterns, and a limited number of PRRs is sufficient to monitor almost all microbial pathogens [17]. The interactions between PRRs and pathogen-associated molecular patterns (PAMPs) activate the host defense system by inducing a series of immune responses [18], leading to the detoxification, cleavage, and elimination of pathogens [19].

Lectin is a PRR that acts as a cell-surface receptor or soluble protein in circulating body fluids, and it plays a prominent role in autoimmune recognition and the clearance of invasive microbes [20]. Based on differences in their molecular structures and functions, the animal lectins can be divided into C-type, F-type, I-type, L-type, M-type, P-type, R-type, F-box, and chitinase-like lectins, ficolins, calnexin, galectins, and intelectins [21]. Of these lectins, the CTLs are among the most widely studied proteins [22]. Members of the CTL family, which bind to carbohydrate in the presence of Ca^{2+}, play important roles in identification during various biological processes. They share a common structural motif in their extracellular carbohydrate recognition domains

* Corresponding author. Engineering and Technology Research Center of Shellfish Breeding in Liaoning Province, Dalian Ocean University, Dalian, 116023, China.
** Corresponding author. Engineering and Technology Research Center of Shellfish Breeding in Liaoning Province, Dalian Ocean University, Dalian, 116023, China.
E-mail addresses: htnie@dlou.edu.cn (H. Nie), yanxiwu@dlou.edu.cn (X. Yan).

https://doi.org/10.1016/j.fsi.2018.12.033
Received 21 May 2018; Received in revised form 12 December 2018; Accepted 18 December 2018
Available online 19 December 2018
1050-4648/

(CRDs), consisting of 14 constant and 18 highly conserved amino acid residues [23,24]. The various lectins are characterized by different CRDs, which have specific structures to identify specific sugars [22]. C-type lectins that bind glucose via the CRD identify specific oligosaccharides on the bacterial cell surface, and link to circulating host proteins and the extracellular matrix [21,25]. The CRD-mediated combination of the CTLs with a specific sugar structure triggers a series of innate immune responses to the pathogen involved [19], ultimately leading to the elimination of the pathogen [22].

The Manila clam, *Ruditapes philippinarum*, is one of the most commercially important marine bivalves, and is widely distributed along the coasts of China, Japan, and Korea. The world production of *R. philippinarum* was about 4 million tonnes in 2016 [26]. In China, the annual yield of *R. philippinarum* accounts for about 90% of all global production. In its natural habitat, the Manila clam displays shell-color variants, including white, orange, and zebra. These shell-color strains have been selected for several generations for fast growth, strong resistance, and a high survival rate [27]. The selective breeding of the zebra strain of *R. philippinarum* has been conducted since 2005, and a hybrid of the white and zebra strains (white–zebra strain) has been established and selected for shell color, growth, stress resistance, and survival for seven generations [28]. In the past decade, the aquaculture of *R. philippinarum* has been greatly threatened by bacterial, parasite, and environmental stresses [29–31]. In recent years, an increasing number of CTL family members have been reported and it is suggested that the CTLs kill bacteria by aggregating the pathogen and inhibiting bacterial growth [32]. For instance, a C-type lectin from *Eriocheir sinensis* (EsLecB) inhibits microorganismal growth by binding to the microorganisms in a process involving carbohydrate recognition and microbial agglutination [33]. Previous studies have demonstrated that different shell-color strains of *R. philippinarum* display a different resistance to environmental stressors [27]. However, the molecular mechanisms underlying the immune roles of clam lectins in the different color strains is unclear.

In this study, we determined the full-length cDNA of a new CTL (RpCTL) and isolated the inducible *RpCTL* gene with molecular biological methods. The time-course of the mRNA expression profile of the *RpCTL* gene was investigated in different strains of *R. philippinarum* after lipopolysaccharides (LPS) stimulation, using fluorescent real-time quantitative PCR (qPCR). The purpose of this study was to understand the immune defense mechanism of *R. philippinarum*, and to provide useful information for its genetic improvement and breeding for disease resistance.

2. Materials and methods

2.1. Experimental Manila clams

Three shell-color strains (zebra strain, white strain, and white–zebra strain) and two populations (cultured population and wild population) of *R. philippinarum* were used in the experiment. The white strain features a white shell color and a high growth rate, and was established with three generations of mass selection. The zebra strain is the product of seven generations of selection and features a zebra-striped shell and a high survival rate. The cultured population and wild population of *R. philippinarum* were collected from Zhuanghe and Dalian, China, respectively. All the Manila clams were acclimatized in aerated seawater (30 psμ) at 22 °C for 7 days before the experiment. The clams had an average shell length of 22.2 ± 1.02 mm and an average weight of 5.4 ± 0.8 g. The temperature and pH of the seawater were 21–23 °C and 7.4–7.6, respectively, during the experiment. The clams were divided into five groups according to their shell color or origin, and were cultured in rectangular storage tanks (20 L).

2.2. Tissue collection after LPS injection

To simulate bacterial challenge, the three shell-color strains and two populations of clams were each divided to two groups. The treatment groups (each population, $n = 30$) were injected into the sinusoid with approximately 50 μl of LPS (100 μg/ml). The control group (each population, $n = 30$) received 50 μl of phosphate-buffered saline (PBS: KH_2PO_4 0.24 g, Na_2HPO_4 1.44 g). Three individuals from of each strain and population in both the treatment and control groups were randomly sampled at different times (3, 6, 12, 24, 48, and 72 h) after LPS challenge or PBS control treatment.

Different tissues, including the hepatopancreas, adductor muscle, gill, siphon, mantle, and foot, were collected from the blank control group to determine the tissue distribution of CTL. Tissue samples, including the gill, siphon, and mantle, were also collected from the PBS-treated control and LPS-challenged groups. The tissues were immediately frozen in liquid nitrogen and stored at −80 °C before analysis [34].

2.3. RNA extraction and cloning the full-length CTL cDNA

Total RNA was extracted using TRIzol Reagent (TRIzol® Plus RNA Purification Kit, Invitrogen, Carlsbad, CA, USA), according to the manufacture's protocol. The total RNA concentration was measured with a NanoDrop 2000c UV/Vis spectrophotometer (Thermo Scientific, Madison, NY, USA). The quality of the total RNA was determined by electrophoresis on a 1% agarose gel. The total RNA was extracted from each tissues of *R. philippinarum*, reverse-transcribed to cDNA, and stored at −20 °C before analysis.

Specific primers were designed based on the CTL (*RpCTL*) gene in the genomic DNA of *R. philippinarum* (Table 1) to generate the full-length cDNA of RpCTL using the rapid amplification of cDNA ends (RACE) (SMARTer™ RACE cDNA Amplification Kit, Clontech). The PCR cycling program was: five cycles of 94 °C for 30 s, and 72 °C for 3 min;

Table 1
Primer sequence used in this study.

Primers name	Sequences(5'-3')
cDNA cloning	
5'RACE	GCTTTCTATTCTAACAAGGTCGCCGCTG
3'RACE	AGAGGGGATGAGGATTGTGGCGAGA
Longup	CTAATACGACTCACTATAGGGCAAGCAGTGGTATCAACGCAGAGT
Shortup	CTAATACGACTCACTATAGGGC
qRT-PCR	
CTL1F	AGATTGATCAGCGGCGACCTTG
CTL1R	CCTTCTGCGTGTCATCCAGTCC
β-actinF	CTCCTGCTTGCTGATCCACATC
β-actinR	GCATCCACGAGACCACTTACA
Prokaryotic expression	
RpCTL-F	ACGCGTCGACTCTACAAGAAATGTTCGAAAT
RpCTL-R	ATAAGAATGCGGCCGCAAGCAGTTTCACTATTTC

five cycles of 94 °C for 30 s, 70 °C for 30 s, and 72 °C for 2 min; 20 cycles of 94 °C for 30 s, 68 °C for 30 s, and 72 °C for 2 min; and finally, 72 °C for 10 min. The PCR fragment of the expected sizes was purified with gel electrophoresis and cloned into the pMD18-T Simple Vector (Takara, Japan) to construct the recombinant plasmid. After *Escherichia coli* Top10 cells (Tiangen) were transformed with this vector, eight positive clones were sequenced. The CTL sequence was confirmed by comparison with CTLs from other vertebrates and invertebrates in the GenBank database of the National Center for Biotechnology Information (NCBI) using the online BLAST procedure.

2.4. Sequence and phylogenetic analyses

The cDNA and amino acid sequences of RpCTL were analyzed with the BLAST algorithm at the NCBI website (http://www.ncbi.nlm.nih.gov/blast). The protein domain features were determined with the Simple Modular Architecture Research Tool (SMART; http://smart.embl-heidelberg.de/). The domain search and annotation were conducted with SMART (http://smart.emblheidelberg.de/). The amino acid sequence of the lectin identified in *R. philippinarum* was compared with a multiple-sequence alignment in BioEdit. A phylogenetic tree was constructed with the MEGA 5.0 software using the neighbor-joining (NJ) method based on this alignment [35], and the reliability of the branching orders was evaluated with bootstrapping ($n = 1000$).

2.5. Expression analysis of RpCTL in different tissues and the time course of gene expression after LPS challenge

For the tissue expression analysis, the mantle, gill, adductor muscle, mantle, hepatopancreas, and foot tissues were collected from three unchallenged clams in the populations of cultured clams, wild clams, white clams, zebra calms, and white–zebra clams, and the total RNA was extracted with TRIzol Reagent (Invitrogen). The first-strand cDNA was synthesized with the Quantitect® Reverse Transcription Kit (TaKaRa), according to the manufacturer's instructions. The synthesized cDNA template was diluted 1:9 for SYBR real-time fluorescent qPCR.

qPCR was performed with the Real-time Detection System (Roche 480) using the SYBR ExScript qRT Kit (TaKaRa), in a total volume of 20 μl, which included 10 μL of SYBR® Primix Ex Taq II (2×), 0.8 μl of each primer, 2 μl of cDNA, and 6.4 μl of H_2O. The thermal cycling protocol used was 94 °C for 5 min, and 40 cycles of 94 °C for 30 s, 60 °C for 30 s, and 72 °C for 30 s. The expression of *RpCTL* mRNA was normalized to that of β-actin mRNA, and the quantitative differences in expression between the different samples was calculated with the $2^{-\Delta\Delta CT}$ method [36]. The gills and hepatopancreas were collected to analyze the temporal expression profiles of *RpCTL* after challenge with LPS. All relative mRNA expression data are given as means ± standard errors ($n = 3$). Differences were considered significant at $P < 0.05$.

2.6. Expression and purification of recombinant RpCTL

The Primer Premier 5.0 software was used to design the gene-specific primers RpCTL-F and RpCTL-R (Table 1) to amplify the complete open reading frame (ORF) of *RpCTL*. The PCR product was purified with the SanPrep Column PCR Product Purification Kit (Sangon), sequenced, and then ligated into the pEASY-T1 Vector (TransGen) to generate pEASY-T1-RpCTL. *Escherichia coli* Trans5α Chemically Competent Cells (TransGen Biotech) were transformed with the plasmid to amplify the ORF fragment. pEASY-T1-RpCTL and pET-30a (Novagen) were digested completely with restriction enzymes *Sal*I and *Not*I (TaKaRa), purified with the SanPrep Column PCR Product Purification Kit (Sangon), and then ligated with T4 DNA ligase (TransGen) at 37 °C for 4 h to construct the recombinant expression vector pET-30a-RpCTL. The recombinant vector was sequenced by Sangon, digested with the *Sal*I and *Not*I enzymes, and confirmed with PCR.

Transetta(D3) Chemically Competent Cells (TransGen Biotech) were transformed with the recombinant expression plasmid pET-30a-RpCTL and cultured overnight at 37 °C. Positive transformants were selected to examine their expression of the recombinant protein. The plasmid was sequenced to ensure the correct insertion of the ORF, and the positive and negative transformants were cultured in LB medium (containing 500 mg/ml kanamycin) at 37 °C with shaking at 200 rpm. When an optical density at a wavelength of 600 nm (OD_{600}) reached 0.4–0.6 (about 2 h), isopropyl β-D-1-thiogalactopyranoside (IPTG) was added to the culture medium at a final concentration of 1 mmol/l, and the culture was incubated for a further 4 h under the same conditions. The cells were collected by centrifugation (700 × g, 15 min) and sonicated on ice until the sample was clarified to the maximum extent. The harvested pellet and supernatant were mixed with 5 × loading buffer, and the RpCTL protein expressed was deduced from its position on a 12% SDS-PAGE gel. The precipitate was harvested and resuspended in binding buffer. The lysate was loaded onto an Ni-NTA HisTrap™ FF Crude column (Sangon), according to the manufacturer's instructions, and then washed with imidazole-eluting buffer (20 mM Tris-HCl, 50 mM NaCl, 8 M urea, x mM imidazole [x = 20, 50, 80, 100, 150, 200, or 300] at 2 ml/min. The eluate solution was collected and analyzed on a 12% gel with SDS-PAGE. The RpCTL protein was renatured with dialysis through graded concentrations of urea, the RpCTL was packed into the treated dialysis bag and immersed sequentially in 2 L beakers containing graded concentrations of urea buffer solution (6, 5, 4, 3, 2, 1, and 0 M urea in 20 mM Tris-HCl, 50 mM Nacl). The dialysate was changed every 12 h until 0 mM was reached. The RpCTL was transferred to PBS for dialysis and the protein concentration was measured.

2.7. Antimicrobial activity assays

The antimicrobial activities of RpCTL against Gram-positive bacteria (*Staphylococcus aureus* and *Bacillus subtilis*) and Gram-negative bacteria (*E. coli* and *V. anguillarum*) were determined. The microorganism were cultured on agar plates and four holes with diameters of 8 mm were drilled in the agar. Then purified RpCTL protein (0.7 μg/ml, 200 μl) or ampicillin (0.5 μg/ml, 20 μl) was then added to the holes, and PBS and recombinant *Schistosoma japonicum* Katsurada thioredoxin (rTrx) were used as the negative controls. The plates were incubated in at 37 °C for 14 h.

The growth curves of the Gram-positive bacterium *B. subtilis* and Gram-negative bacterium *E. coli* cultured with RpCTL were constructed as follows. A single colony of *B. subtilis* or *E. coli* was selected and transferred into 5 ml of LB medium. Purified RpCTL protein was added to the medium to a final concentration of 0, 20, 60, or 180 μg/ml. An equal volume of PBS was used as the negative control. The samples were incubated at a temperature of 37 °C with shaking at 200 rpm, and the OD_{600} was measured every 2 h, the samples were analyzed in three separate experiments.

2.8. Survival rate of R. philippinarum after infection with V. anguillarum and injection of RpCTL

Clams were collected from Jinshitan, Dalian, divided into four groups with 50 clams in each group, and maintained for a week. The first and second groups were injected with 0.9 μg/μl RpCTL (50 μl), and the third and fourth groups with the same volume of PBS as the control groups. After 1 h, 50 μl of *V. anguillarum* ($OD_{600} = 0.1$) was injected into the first and the third groups. The second and fourth groups were injected with the same volume of PBS as the controls. The number of clams surviving in each group was counted every 12 h after infection. The survival rate was equal to (surviving clams/50) × 100%, and the survival rate curves were constructed from these data.

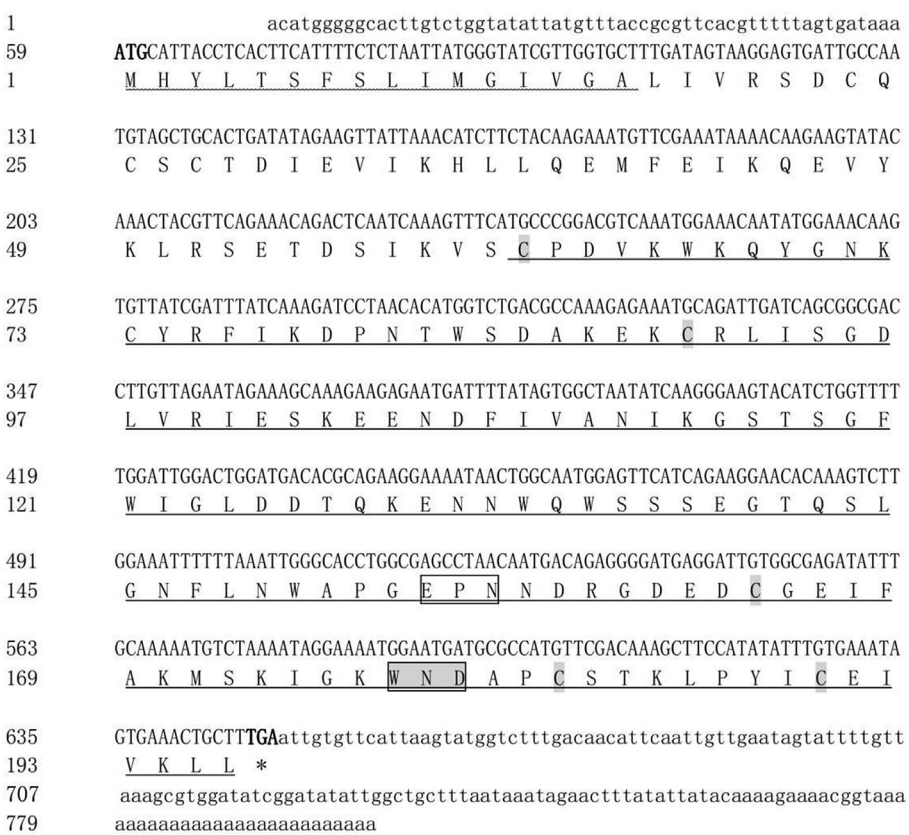

Fig. 1. Nucleotide and deduced amino acid sequences of *R. philippinarum* C-type lectin. The full sequence of *RpCTL* is 802 bp, with a 591-bp ORF encoding a 196-amino-acid protein, a 58-bp 5′ untranslated region (UTR), and a 153-bp 3′ UTR. The predicted signal peptide (amino acids 1–16) is underlined in bold line. The first methionine (M) is considered the first deduced amino acid. The putative CRD (amino acids 61–196) is underlined. The EPN motif, which is important in determining the ligand-binding specificity, is boxed. The WND motif, which contains the Ca^{2+}-binding site, is boxed and shaded in gray. Conserved cysteine residues are shown in gray.

3. Results

3.1. cDNA cloning and sequence analysis of RpCTL

The cDNA sequence of the *RpCTL* gene of *R. philippinarum* was determined and deposited in GenBank (accession number: MH368785). The full-length cDNA of *RpCTL* was 802 bp, and consisted of a 5′ untranslated region (UTR) of 58 bp, a 3′ UTR of 153 bp (including the poly (A) tail signal), and an ORF of 591 bp, including the stop codon (TGA) (Fig. 1). The ORF encoded a polypeptide of 196 amino acids with an isoelectric point of 5.19 and a predicted molecular weight of 22.36 kDa. An analysis with the SMART program predicted that the deduced amino acid sequence of RpCTL has a signal peptide of 16 amino acid residues and a single RpCTL CRD. Several important signatures of the CTL family were detected in RpCTL: the four completely conserved cysteine residues (Cys^{30}–Cys^{104}, Cys^{124}–Cys^{132}) involved in the formation of the internal CRD disulfide bonds and the EPD (Glu^{94} –Pro^{95} –Asn^{96}) motif, which determines the specificity of ligand binding (Fig. 1).

3.2. Homology and phylogenetic analyses

A multiple alignment of CRD amino acid sequences showed that the CRD of RpCTL is consistent with those of other species CTLs that contain six conserved cysteine residues. Four cysteine residues (Cys^{30}, Cys^{104}, Cys^{124}, Cys^{132}) are involved in forming the internal disulfide bonds that are highly conserved in the CRD. Two Ca^{2+}-dependent carbohydrate-binding motifs, EPN (Glu^{94}–Pro^{95}–Asn^{96}) and WND (Trp^{119}–Asn^{120}–Asp^{121}), were also detected in RpCTL. A phylogenetic analysis of the CRD amino acid sequences of RpCTL and those of other species was performed (Fig. 2).

To evaluate the molecular evolutionary relationships between RpCTL and other CTLs, a phylogenetic tree was constructed with the NJ algorithm (1000 bootstrap replications) based on the amino acid sequences of 18 CTLs (Fig. 3). An analysis of RpCTL and the CTLs of other species with BLASTp showed that RpCTL shares 33%–40% identity with those of other species. As shown in Fig. 3, RpCTL clustered most closely with the CTLs of *Crassostrea virginica* and *C. gigas*, and then with those of other mollusks, including *Azumapecten farreri*, *Haliotis discus discus*, and *Meretrix meretrix*. The vertebrate CTLs formed another cluster, including the fish CTLs (*Anguilla luzonensis*, *Paralichthys olivaceus*, *Perca flavescens*, and *Spirinchus lanceolatus*), mammal CTLs (*Homo sapiens* and *Mus musculus*), amphibian CTL (*Xenopus tropicalis*), and bird CTL (*Apaloderma vittatum*). The CTLs of other crustacean invertebrates (*Penaeus monodon* and *Marsupenaeus japonicus*) formed a third cluster. Thus, the phylogenetic relationships of RpCTL amino acid sequence are consistent with the traditional classification of the clam.

3.3. RpCTL mRNA expression profiles in different tissues

The expression of *RpCTL* mRNA in different tissues was measured with qPCR, using β-actin as the housekeeping-gene control. In this study, the *RpCTL* transcripts were widely expressed in the various tissues of the different strains, including in the mantle, gill, siphon, adductor muscle, hepatopancreas, and foot. In the cultured clams, the expression of *RpCTL* was significantly higher in the siphon (4.38-fold), gill (7.44-fold), and hepatopancreas (11.52-fold) than in the foot ($P < 0.05$), whereas the expression was lower in the mantle (0.17-fold) and adductor muscle (0.78-fold) than in the foot ($P > 0.05$) (Fig. 4). In the wild clams, the *RpCTL* transcripts were 3.89-, 4.16-, and 49.00-fold higher in the gill, siphon, and hepatopancreas, respectively, than in the foot ($P < 0.05$). *RpCTL* expression was lower in the mantle (0.50-fold) and adductor muscle (0.09-fold) than in the foot ($P > 0.05$) (Fig. 4). In the white clams, *RpCTL* was highly expressed in the mantle, gill, siphon, and hepatopancreas (5.70-, 12.24-, 3.21-, and 40.72-fold higher than in the foot, respectively; $P < 0.05$), whereas its expression was lower in the adductor muscle (2.08-fold) than in the foot ($P > 0.05$) (Fig. 4). In the white–zebra clam, *RpCTL* was highly expressed in the gill, siphon, and hepatopancreas, at 3.79-, 6.83-, and 13.67-fold higher than in the

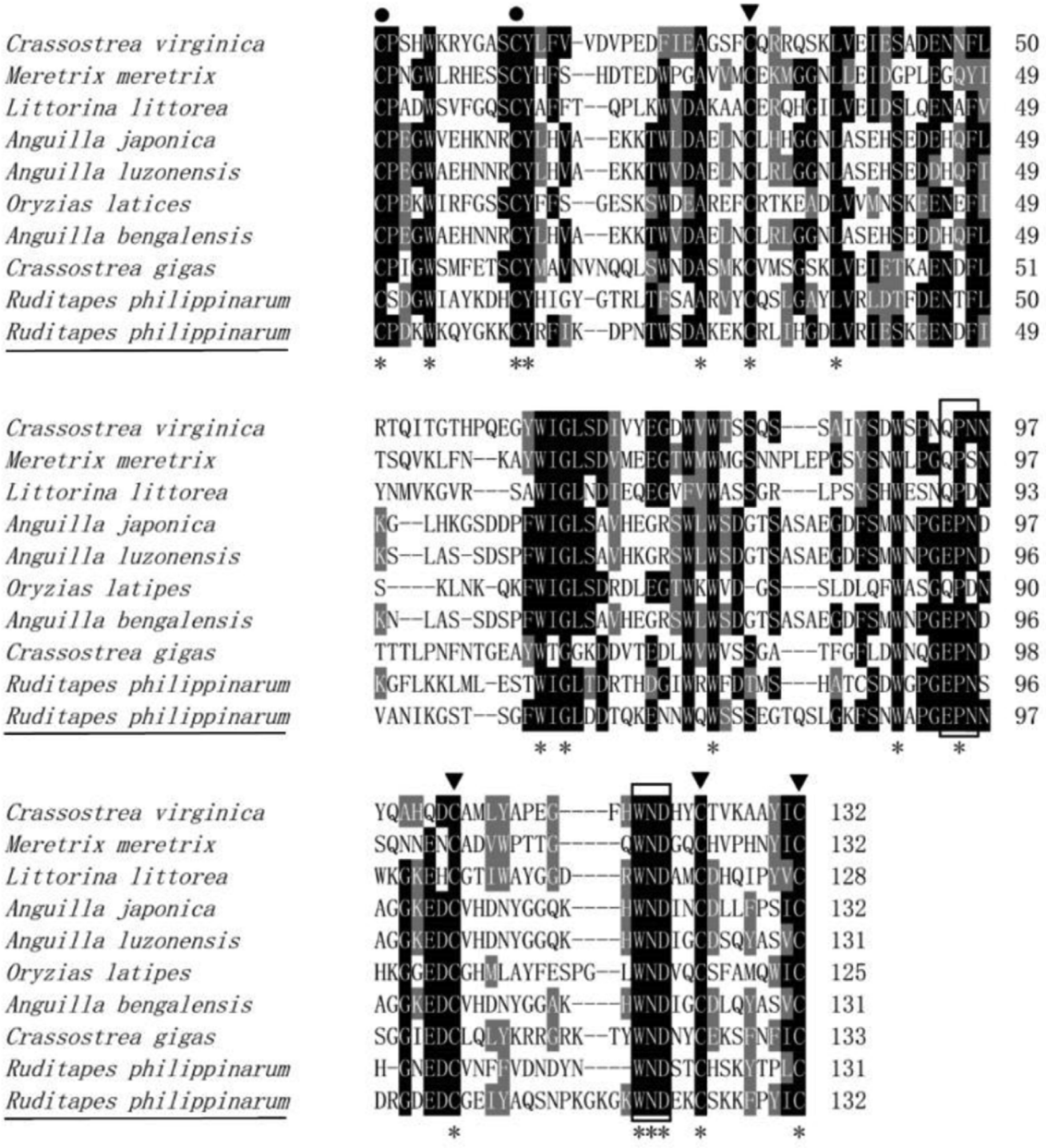

Fig. 2. Alignment of CRD amino acid sequences of RpCTL from *R. philippinarum* and CTLs of other species. Identical and similar amino acids are shaded in black and gray, respectively. The EPN and WND motifs, which determine the carbohydrate-binding specificity, are highlighted in boxes. The four cysteine residues involved in the formation of two conserved inner disulfide bonds are labeled with ● Two extra cysteine residues at the N-terminus are marked with ▼.The GenBank accession numbers of the aligned sequences are: *Crassostrea virginica* (XP_022287105.1), *Meretrix meretrix* (ANG56319.1), *Littorina littorea* (AJA37872.1), *Anguilla japonica* (BAU79657.1), *Anguilla luzonensis* (BAU79658.1), *Oryzias latipes* (XP_020568824.1), *Anguilla bengalensis bengalensis* (BAU79649.1), *Crassostrea gigas* (EKC30692.1), *Ruditapes philippinarum* (ACU83213.1), and *Azumapecten farreri* (AAT77680.1).

foot, respectively ($P < 0.05$). In the zebra clam, its expression was 4.68- and 17.64-fold higher in the gill and hepatopancreas, respectively, than in the foot ($P < 0.05$), but lower in the mantle (0.04-fold) and adductor muscle (0.78-fold) than in the foot ($P > 0.05$) (Fig. 4).

3.4. Variation in RpCTL expression in gills and hepatopancreas of R. philippinarum after LPS infection

The transcriptional profiles of *RpCTL* in the gills and hepatopancreas over time after LPS injection are shown in Fig. 5. *RpCTL* expression showed an upregulated trend in the cultured clams after LPS injection. In the gills of the cultured clams, the expression was significantly upregulated 5.42- and 5.28-fold ($P < 0.05$) at 3 and 6 h compared with the PBS-injected controls, and 0.56-fold and 3.35-fold at 12 and 24 h postinjection ($P < 0.05$). It decreased to 0.48-fold at 48 h, and was then upregulated again at 72 h to 3.40-fold higher than the control group value ($P < 0.05$) (Fig. 5A). Similarly, the CTL transcripts were increased in the hepatopancreas at 3 and 6 h to 19.02- and 12.41-fold higher than those in the control group ($P < 0.05$), and were maintained at similar levels until 6 h postinjection. They decreased to 2.07- and 0.87-fold higher than the control level ($P > 0.05$) at 12 and 24 h, slowly increased to 2.29-fold higher ($P > 0.05$) at 48 h postinfection, and then peaked at 248.33-fold higher ($P < 0.05$) than the control group at 72 h after LPS injection (Fig. 5B).

In the wild clams, *RpCTL* showed different expression patterns in these two tissues after LPS injection. The expression of *RpCTL* in the gill of the wild clams tended to increase after LPS injection, and was significantly (3.18-fold) higher than the control level ($P < 0.05$) at 3 h

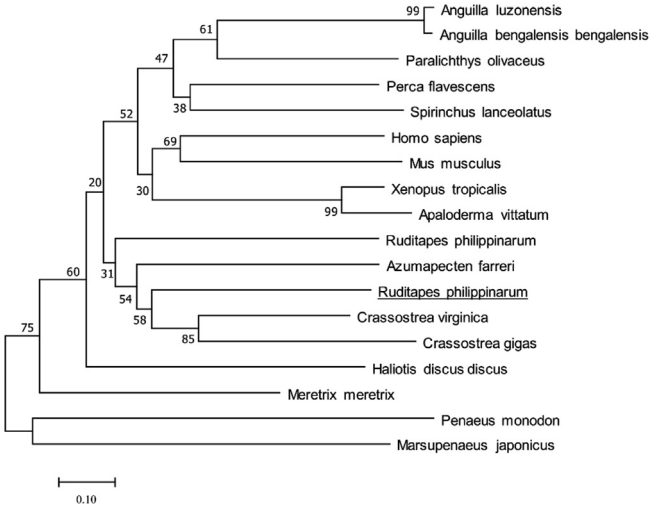

Fig. 3. Phylogenetic tree of *R. philippinarum* C-type lectin and those of other species, based on the CRD sequences, was constructed with the MEGA 5.0 software using the neighbor-joining method. The *R. philippinarum* C-type lectin identified in this study is underlined. Numbers shown at the forks indicate the percentage bootstrap values calculated from 1000 replicates. The accession numbers of the protein sequences used in the phylogenic analysis are: *Anguilla luzonensis* (BAU79658.1), *Anguilla bengalensis bengalensis* (BAU79649.1), *Paralichthys olivaceus* (ACY70392), *Xenopus tropicalis* (XP_002932255), *Apaloderma vittatum* (XP_009872314), *Homo sapiens* (NP_006335), *Mus musculus* (NP_058031), *R. philippinarum* (ACU83213.1), *Meretrix meretrix* (ANG56319.1), *Haliotis discus discus* (ABO26594), *Crassostrea virginica* (XP_022290415.1), *Marsupenaeus japonicus* (ADG85667.1), *Crassostrea gigas* (EKC18650.1), *Perca flavescens* (ACO82036.1), *Spirinchus lanceolatus* (BAE45334.1), and *Penaeus monodon* (AAZ29608.1).

after LPS injection. It then decreased sharply to 0.32-fold ($P < 0.05$) at 6 h, and peaked at 12 h at 91.85-fold ($P < 0.05$); it then decreased again to 2.55-, 1.64-, and 1.89-fold ($P < 0.05$) at 24, 48, and 72 h after injection, respectively (Fig. 5C). *RpCTL* expression in the hepatopancreas was significantly affected at the different time points after LPS challenge. *RpCTL* transcripts decreased to 0.47-fold of the control level ($P < 0.05$) at 3 h, and then increased at 6 and 12 h (to 1.56- and 2.82-fold, respectively; $P < 0.05$) (Fig. 5D). However, its upregulation was maximal at 12 h, at 4.43-fold higher than the control level ($P < 0.05$). It decreased thereafter to its original level (0.74-fold higher than the control level, $P < 0.05$) at 48 h and remained at this level (1.16-fold, $P < 0.05$) up to 72 h (Fig. 5D).

In this study, we also analyzed the temporal expression of *RpCTL* in the white clam, zebra clam, and white–zebra clam after LPS treatment. Our results show that *RpCTL* transcript expression was first upregulated and then downregulated in both the gill and hepatopancreas of the white clam after LPS injection. It increased significantly in the gill of the white clam at 3, 6, and 12 h (3.34-, 3.67-, and 3.72-fold higher than the control, respectively; $P < 0.05$), and then increased rapidly to 24 h after LPS injection (44.40-fold higher than the control; $P < 0.05$), decreased suddenly at 48 h (Fig. 5E). However, the hepatopancreas showed a different expression patterns than the gill after LPS injection. The expression of *RpCTL* in the hepatopancreas was significantly elevated at 3 h (3.21-fold higher than the control group; $P < 0.05$), but decreased at 6 h, after which it increased rapidly at 12 h and 24 h after LPS injection (2.68- and 1.86-fold higher than the control, respectively). It then decreased sharply to 0.13-fold higher than the control value ($P < 0.05$) at 48 h (Fig. 5F).

Our results indicated that *RpCTL* mRNA was highly expressed in the gill and hepatopancreas in healthy white–zebra clams. After LPS injection, the transcription of *RpCTL* increased in both the gill and hepatopancreas to 2.26-fold ($P < 0.05$), higher than in the control group. It then suddenly decreased to its original level at 6 h. It increased again at 12, 24, and 48 h (especially after 24 and 48 h), peaking at 3.70-fold higher than the control at 48 h (Fig. 5G). The transcription of *RpCTL* in the hepatopancreas of the white–zebra clams was upregulated at 3 h after LPS injection, when it was 6.63-fold higher than the control level ($P < 0.05$), but decreased sharply to 0.07-fold of the control level ($P < 0.05$) at 6 h. It then increased significantly, peaking at 12 h after LPS injection, when it was 28.49-fold higher than the control level. It decreased to 8.85- and 6.41-fold higher than the control level ($P < 0.05$) at 24 and 48 h, respectively (Fig. 5H).

The expression of *RpCTL* in the gill and hepatopancreas of the zebra clams also showed a different time course after LPS injection. In the gill, *RpCTL* transcripts were significantly increased at 3 and 6 h after injection (peak) to 4.66- and 5.02-fold higher than the control level, respectively ($P < 0.05$). They then decreased significantly at 12 and 24 h

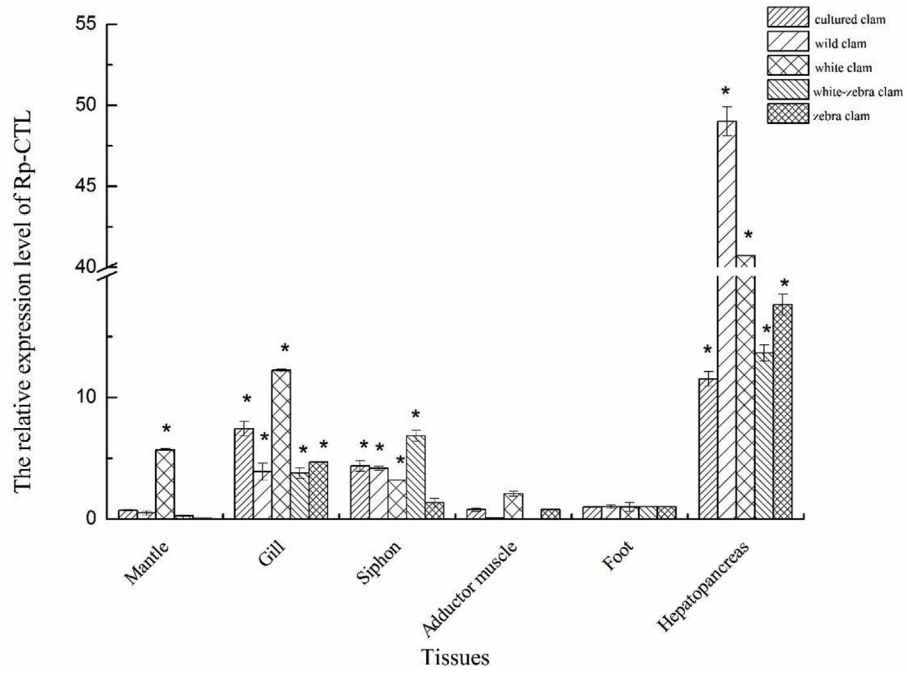

Fig. 4. Relative expression of C-type lectin mRNA in different tissues of *R. philippinarum* detected with real-time PCR. The β-actin gene of *R. philippinarum* was used as the internal control. C-type lectin transcript levels in the mantle, gill, siphon, adductor muscle, foot, and hepatopancreas. Data are expressed relative to the expression of the C-type lectin mRNA in the foot. Data are shown as means ± S.E. ($n = 3$). *$P < 0.05$.

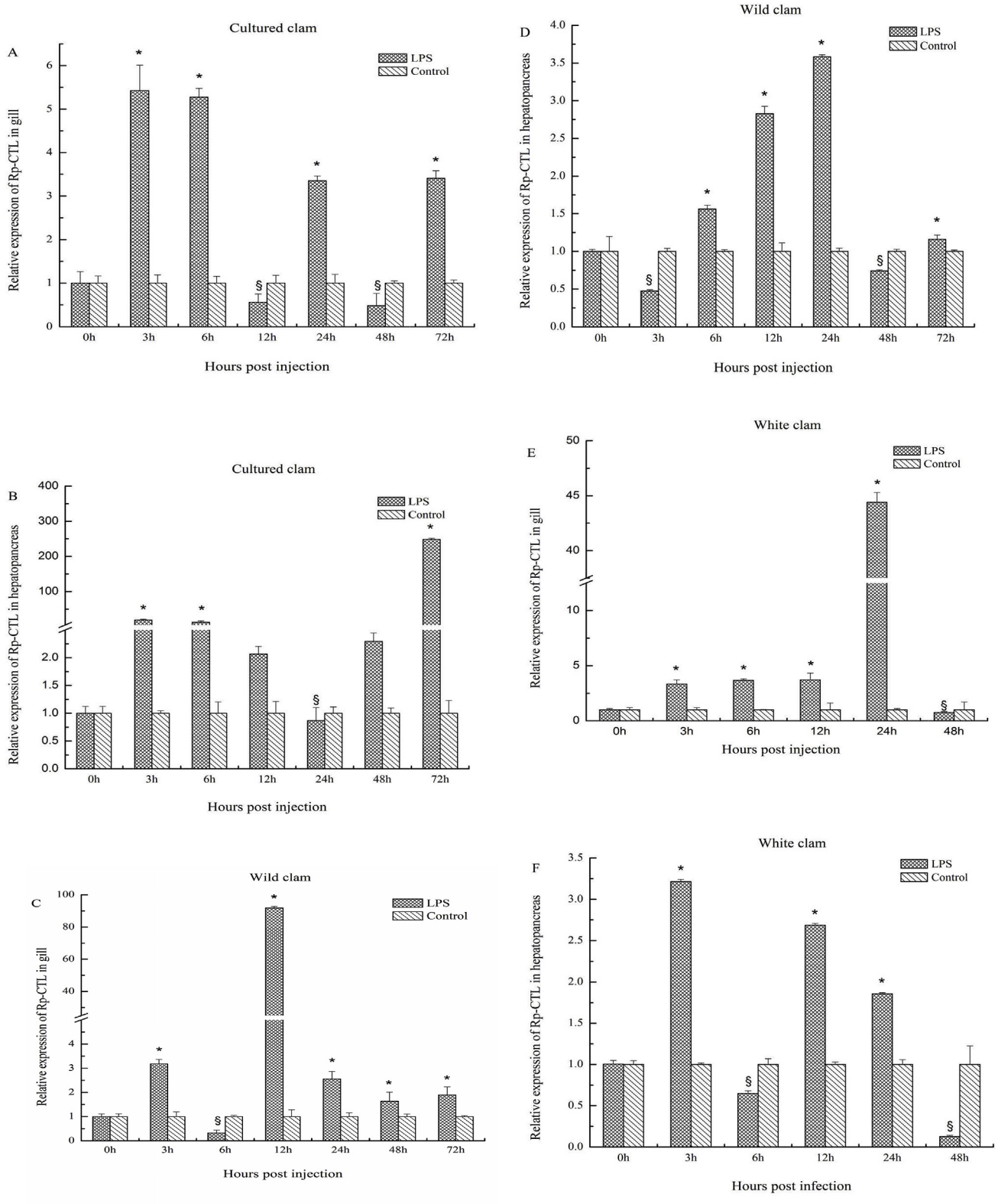

Fig. 5. Expression analysis of C-type lectin in *R. philippinarum* gill and hepatopancreatic tissues (from cultured clams, wild clams, white clams, zebra clams, and white–zebra clams) in response to LPS injection. Expression was determined with real-time PCR relative to β-actin mRNA expression at 3, 6, 12, 24, and 48 h after challenge with LPS (black bars) or PBS (control white bars), in the two groups of C-type lectin. Expression in the control group was set at 1. The expression of C-type lectin was significantly increased after LPS treatment (black bars). Significant differences relative to the control value ($P < 0.05$) are shown as * (significantly increased) and § (significantly reduced). Data are shown as means ± S.E. ($n = 3$).

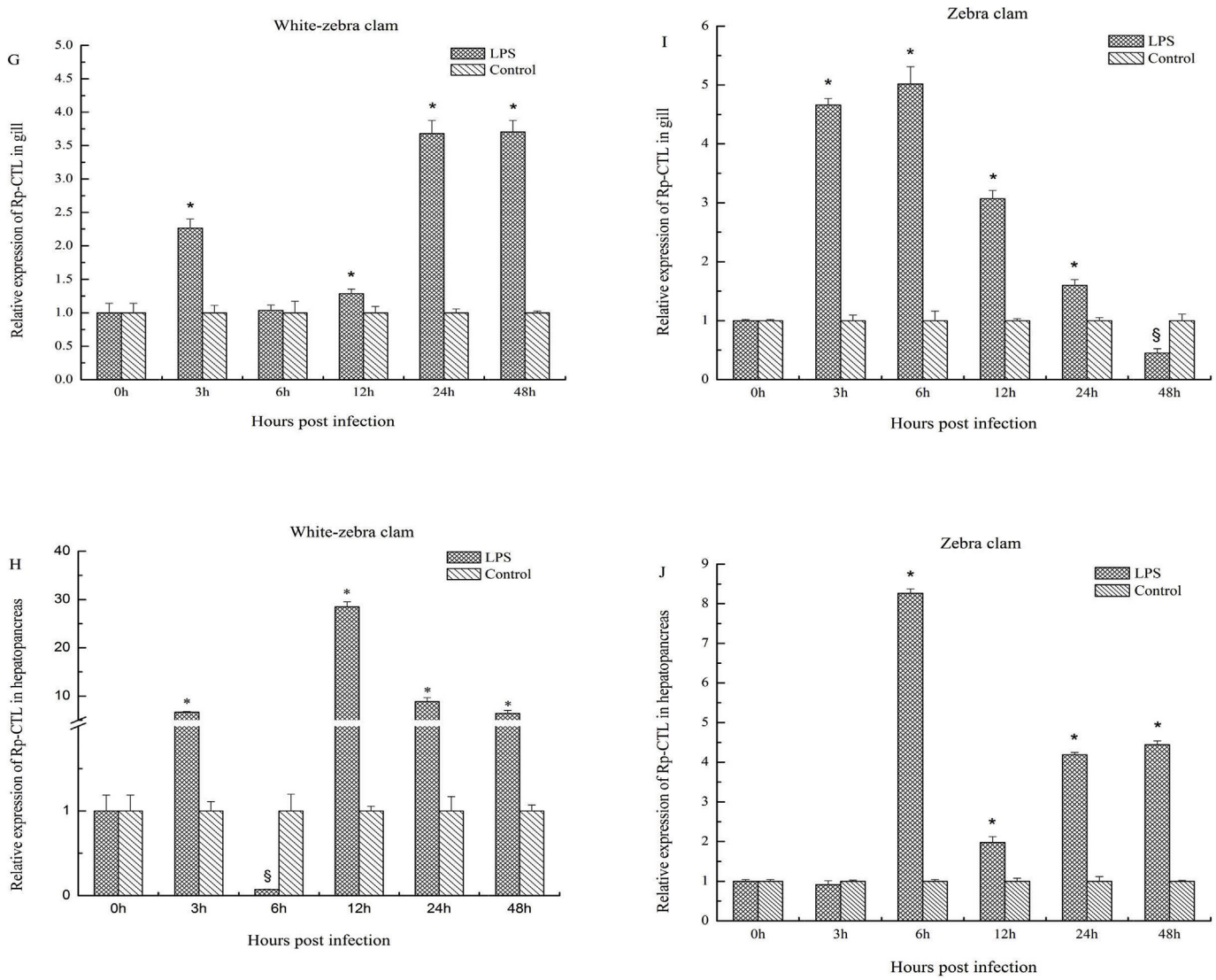

Fig. 5. (*continued*)

after LPS injection to 3.07- and 1.60-fold higher than the control level, respectively, and then decreased sharply to 0.45-fold of the control level ($P < 0.05$) at 48 h (Fig. 5I). The expression profile in the hepatopancreas was similar to that in the gills after LPS injection. *RpCTL* transcription peaked at 6 h, at 8.26-fold higher than the control level ($P < 0.05$), but decreased sharply at 12 h to 1.97-fold higher than the control level ($P < 0.05$). It then it increased at 24 h (4.18-fold higher than the control level; $P < 0.05$) and remained at that level until 48 h (4.44-fold higher than the control level; $P < 0.05$) (Fig. 5J).

3.5. Expression and purification of recombinant RpCTL

The recombinant RpCTL protein was expressed in the pET-30a system. The molecular weight of RpCTL was predicted to be about 22.36 kDa and the predicted PI was 5.19. In a prokaryotic expression system, RpCTL was expressed as a fusion protein with a His-tag at its N-terminus, and had an apparent molecular mass of 23 kDa. Whole-cell lysates of Transetta cells transformed with pET-30a-RpCTL and treated with IPTG were analyzed with 12% SDS-PAGE (Fig. 6A). Compared with noninduced Transetta cells (Fig. 6A, lane 1), a thicker band with a molecular weight of 23 kDa (Fig. 6A, lane 2) was observed, consistent with the predicted molecular weight of RpCTL, indicating that RpCTL was successfully expressed (Fig. 6A, lane 2). The fusion protein was purified with Ni–NTA affinity chromatography using different concentrations of imidazole (20, 50, 80, 100, 150, 200, or 300 mM) from the precipitates of Transetta cells. SDS-PAGE showed that the RpCTL concentration was higher after elution with 80, 100, or 150 mM imidazole (Fig. 6B, lane 1–3). A considerable amount of RpCTL was obtained with affinity chromatography on an Ni–NTA column using eluent containing 100 mM imidazole.

3.6. Antimicrobial activity assays

To study the antibacterial activity of RpCTL, its inhibitory effects on the growth of *S. aureus*, *E. coli*, *B. subtilis*, and *V. anguillarum* were studied. RpCTL was compared with the negative controls (PBS and rTrx) in a bacteriostatic circle test. Transparent circular regions were observed around the RpCTL-filled holes in *E. coli*, *V. anguillarum*, *S. aureus* and *B. subtilis* lawns (Fig. 7). These regions were bacteriostatic regions, and larger regions were observed around corresponding holes filled with ampicillin, used as the positive control (Fig. 7). These results confirm the inhibitory effects of RpCTL on *V. anguillarum*, *S. aureus*, *B. subtilis* and *E. coli*. The transparent inhibitory zones on the *E. coli*, *V. anguillarum*, and *S. aureus* plates treated with RpCTL were larger than those on the *B. subtilis* plates, implying that the inhibitory effects of RpCTL on *E. coli*, *V. anguillarum*, and *S. aureus* were stronger than that on *B. subtilis*.

The growth curves for *B. subtilis* and *E. coli* are shown in Fig. 8.

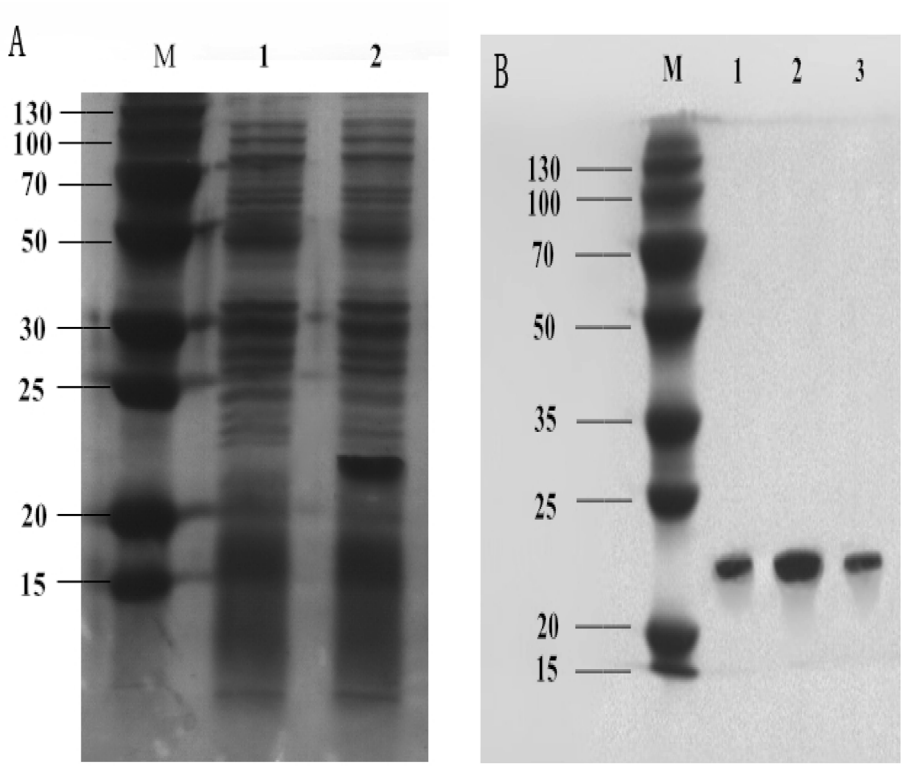

Fig. 6. Expression and purification of RpCTL in bacterial cell lysates, analyzed with SDS-PAGE. A. Lane M: protein molecular standard; lane 1: lysate of *E. coli* Transetta cells transformed with pET-30a without IPTG induction; lane 2: lysate of *E. coli* Transetta cells transformed with pET-30a and induced with 1 mM IPTG at 37 °C. B. Lane M: protein molecular weight standard; lanes 1–3: purified protein eluted with 80 mM, 100 mM, and 130 mM imidazole, respectively.

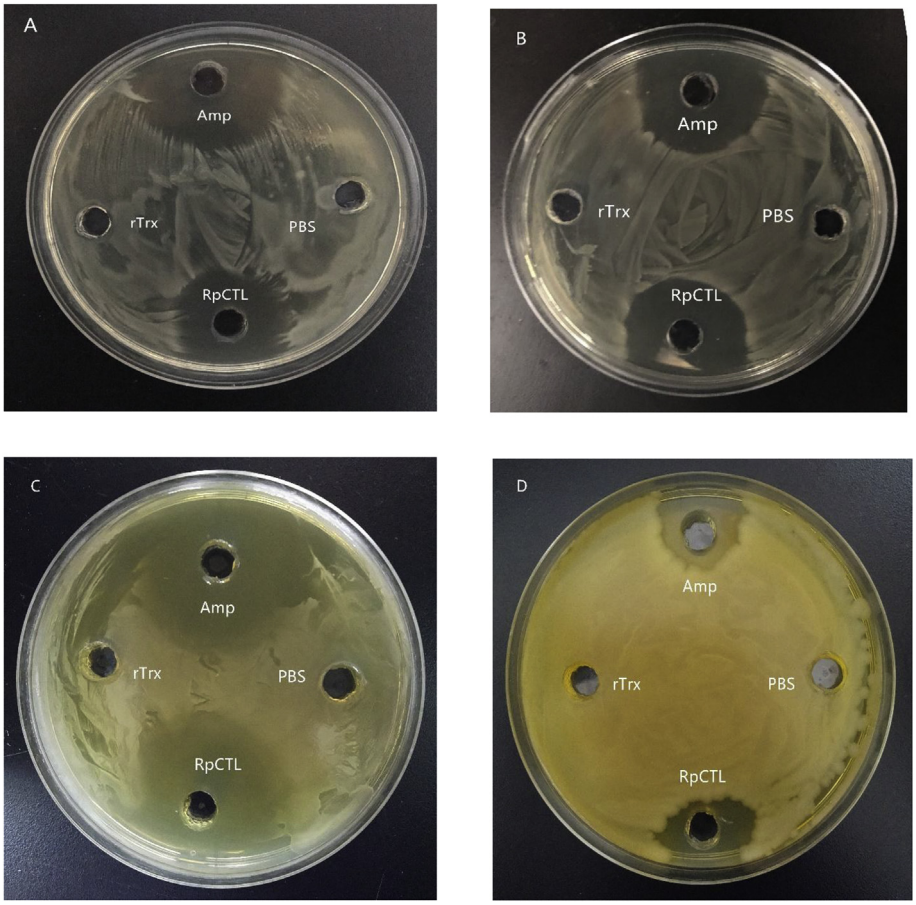

Fig. 7. Microbial killing activity of RpCTL in a bacterial inhibition zone assay. Plate (A): *E. coli*; (B): *V. anguillarum*; (C): *S. aureus*; and (D): *B. subtilis*. Ampicillin was used as the positive control, and rTrx protein and PBS as the negative controls. A clear ring around the hole indicates antibacterial activity.

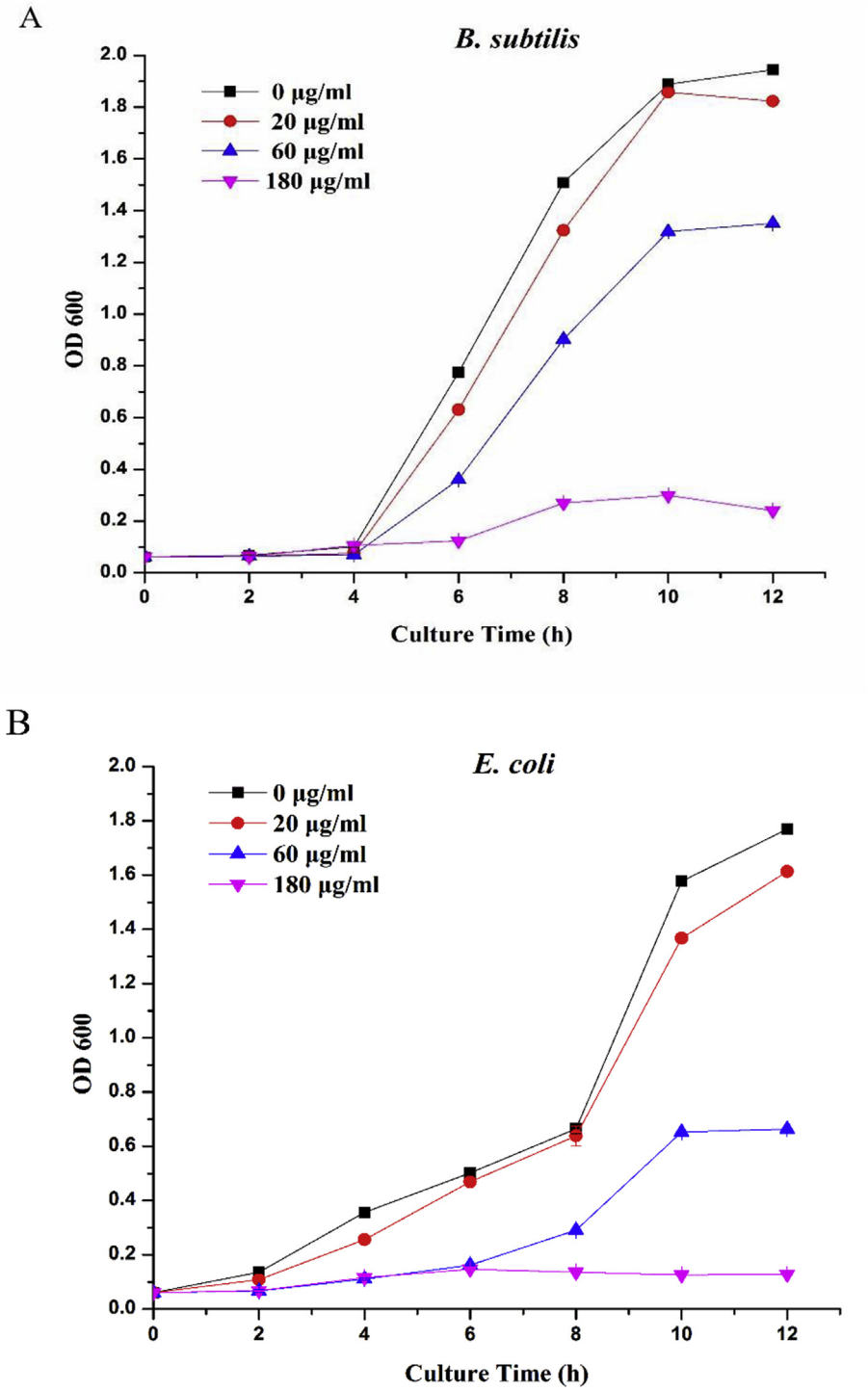

Fig. 8. Growth inhibitory activity of RpCTL against *B. subtilis* and *E. coli*. Each bacterium was suspended in the same volume of LB medium, and RpCTL was added at a concentration of 0, 20, 60, or 180 μg/ml. The culture was incubated in an incubator at 37 °C with shaking at 200 rpm, and the OD_{600} was measured after 2, 4, 6, 8, 10, and 12 h to construct growth curves for the different groups. Bacterial growth curves for *B. subtilis* (A) and *E. coli* (B) are shown.

When the final concentration of RpCTL was 180 μg/ml, the OD_{600} values of both *B. subtilis* and *E. coli* were reduced. Generally, the growth of microorganisms was inhibited at this concentration, whereas the effect of 20 μg/ml RpCTL was weak (Fig. 8A and B). After incubation with 20, 60, or 180 μg/ml RpCTL or the same volume of PBS (as the control group) for 12 h, the *E. coli* OD_{600} increased to 1.36, 0.65, or 0.13, respectively (Fig. 8A), and those of *B. subtilis* were 1.86, 1.32, or 0.30, respectively (Fig. 8B). Thus, the inhibition of *E. coli* by RpCTL was significantly greater than the inhibition of *B. subtilis*, which is consistent with the results of the bacteriostatic circle test (Fig. 7A and D). The inhibition of *E. coli* and *B. subtilis* cell growth by RpCTL at concentrations of 20 and 60 μg/ml was weaker than that at 180 μg/ml RpCTL (Fig. 8A and B).

3.7. Survival rate of *R. philippinarum* after infection with *V. anguillarum* and injection with RpCTL

After clams were injected with RpCTL, they were injected with *V.*

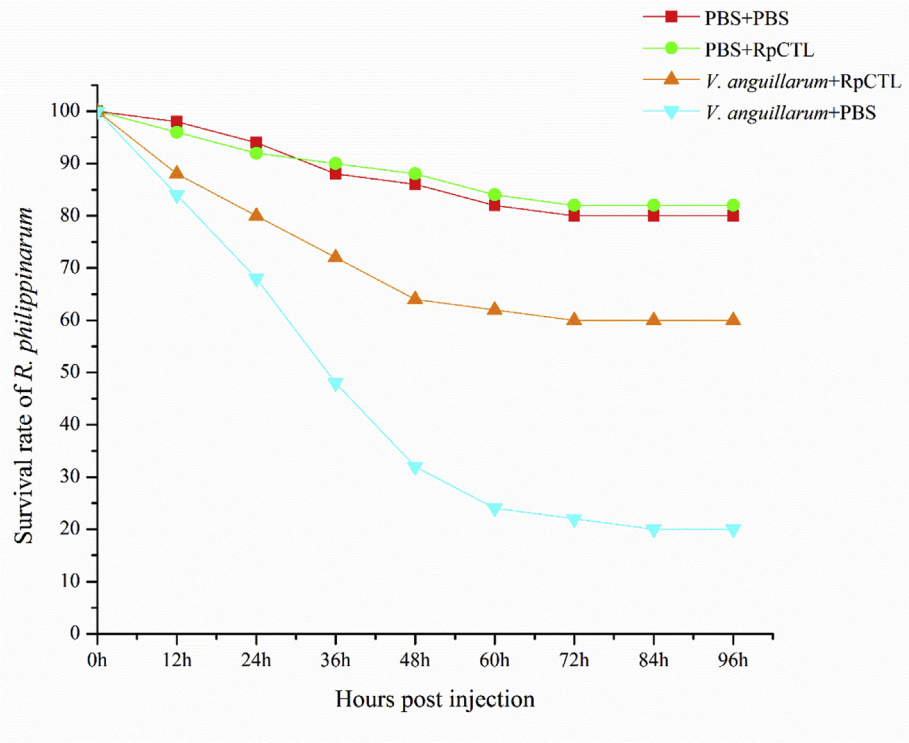

Fig. 9. Survival rate curve of *R. philippinarum* infected with *V. anguillarum* after RpCTL injection. Four groups of *R. philippinarum* were injected with PBS + PBS, PBS + RpCTL, *V. anguillarum* + RpCTL, or *V. anguillarum* + PBS, and their survival rates were calculated every 12 h.

anguillarum, and their survival rates were observed. The survival rate of the clams in each group decreased at 12 h after injection with *V. anguillarum*. This reduction was greatest in the clams injected with PBS and *V. anguillarum*, with a survival rate of 86.8%. The smallest reduction was in the clams injected with PBS and PBS, followed by that in the clams injected with RpCTL and PBS (Fig. 9). The reduction in the survival rate was higher in the RpCTL and *V. anguillarum* groups, the survival rate was stable after 72 h later, and all survival rates were greater than 50% at 72–96 h postinfection. In the clams treated with PBS and *V. anguillarum*, the survival rate continued to decline, reaching 20.4% at 96 h after *V. anguillarum* infection (Fig. 9).

4. Discussion

The identification of infectious pathogens is an important part of the immune response in animals. C-type lectins are the main pattern recognition molecules of the innate immune system [37], and are involved in a series of potential pathogens of congenital immune response of a large part of the multifunctional gene families [38]. Many lectins, such as the glucose-binding proteins, mediate non-self recognition and intercellular interactions via their structure-related Ca^{2+}-dependent CRDs. CTLs have been studied in vertebrates and invertebrates for many years [39]. In this study, the full-length cDNA of a new RpCTL was cloned, which encoded a 196-residue protein with a single CRD. The deduced amino acid sequence indicated that it is relatively well conserved. The CRD containing the Cys^{30}–Cys^{104} and Cys^{124}–Cys^{132} disulfide bonds, the Ca^{2+} binding site EPN (Glu^{94}–Pro^{95}–Asn^{96}), and the WND motif binding site we re also found in RpCTL. The two conserved disulfide bridges maintain the structural stability of the protein. The four cysteine residues in the CRD form a fundamental and stable two-double-loop structure [40]. The N-terminus of the CRD sequence contains two cysteine residues based on the combination of “short” CRD (only four cysteine residues) [40,41], which indicates that the RpCTL CRD is the “long” type, like the CTLS of other fish species [42–44]. RpCTL is predicted to be a transmembrane protein because it contains a classical transmembrane region, but its signal peptide indicates that RpCTL is secreted, suggesting that RpCTL is a membrane receptor that identifies carbohydrate ligands and soluble proteins secreted by defense molecules. This is consistent with the CTL of the Japanese flounder *Paralichthys olivaceus* (JFCTL) [45]. Our results indicate that RpCTL is a new member of the CTL family and may be involved in the immune response of *R. philippinarum* to bacterial attack.

Large numbers of marine mollusk lectins are highly expressed in the gills and hepatopancreas, e.g., CfLec-1 and Cflec-5 from *C. farreri* [9,46] and galectins from *C. virginica* and *A. irradians* [47–49]. In this study, we observed that *RpCTL* was highly expressed in the gills and hepatopancreas of the five groups of *R. philippinarum*. In bivalves, the gill is involved in continuous water exchange, and is therefore susceptible to pathogen infection, and the hepatopancreas is a vital organ in the immune defense of the mollusk [46,50,51]. To understand their functions, it is essential to determine the tissue-specific expression patterns of the agglutinin gene. *RpCTL* is widely expressed throughout the tissues of healthy clams, including the mantle, siphon, adductor muscles, gill, foot, and hepatopancreas.

Although RpCTL recognizes the antigenic glycoprotein of *Listonella anguillarum* [52], the molecular mechanism of LPS recognition by RpCTL in LPS-injected *R. philippinarum* has not been reported. In this study, the expression of *RpCTL* mRNA was significantly affected By LPS injection. For example, the expression of *RpCTL* was upregulated in the gills (at 3, 6, 24, and 72 h after injection with LPS) and hepatopancreas (at 3, 6, and 72 h) of cultured clams ($P < 0.05$). *RpCTL* transcripts were also upregulated in the gills (at 3, 12, 24, 48, and 72 h after injection with LPS) and hepatopancreas (at 3, 12, 24, 48, and 72 h) of wild clams. The expression of *RpCTL* transcripts in the white strain was upregulated in the gill (at 3, 6, 12, and 24 h after injection with LPS) and hepatopancreas (at 3, 12, and 24 h). Similar tends were observed in the white–zebra strain insofar as *RpCTL* transcripts were upregulated in the gills (at 3, 12, 24, and 48 h) and hepatopancreas (at 3, 12, 24, and 48 h) after injection with LPS. In the zebra strain, *RpCTL* expression was upregulated in the gills (at 3, 6, 12, and 24 h) and hepatopancreas (at 6,

12, 24, and 48 h) after LPS injection (Fig. 5). These expression profiles are the same as those as recently reported for *VpCTL* and *SgCTL-1* [52,53]. However, the expression of *RpCTL* also decreased after injection with LPS, e.g., in the gill (12 and 48 h) and hepatopancreas (24 h) in cultured clams, in the gill (6 h) and hepatopancreas (3 and 48 h) in wild clams, in the gill (48 h) and hepatopancreas (6 and 48 h) in the white clam, in the hepatopancreas (6 h) in the white–zebra clam, and in the gill (48 h) in the zebra clam (all $P < 0.05$). A recent study showed a similar expression profile for *SgCTL-1* in *Solen grandis* [53]. In the present study, the expression of *RpCTL* was increased by LPS challenge, and the upregulation of *RpCTL* may minimize the harm caused by bacterial stimulation and the accumulation of negative effects [52]. A recombinant RpCTL protein was expressed in an *E. coli* expression system as an N-terminally His-tagged fusion protein and purified with immobilized metal-ion-affinity chromatography with imidazole as the eluent. An imidazole concentration of 100 mM was selected to purify the RpCTL fusion protein to high purity and in large quantities, and the amount of imidazole was optimized. Previous reports have indicated that CTL participates in an animal's immune response to pathogens. Our results for the RpCTL protein extend our understanding of the CTL functions in shellfish species.

It has been reported that CTL also inhibits bacteria in shrimp. The CTL from the Chinese shrimp *Fenneropenaeus chinensis* (Fc-hsL) has a strong inhibitory effect on Gram-positive bacteria and some fungi, and a moderate inhibitory effect on Gram-negative bacteria [54]. Others studies have shown that FcLec4 of *F. chinensis* has an activity directly that inhibits the growth and even kills *V. anguillarum* in shrimp, and promotes the elimination of *V. anguillarum* in vivo [55]. In the present study, the antimicrobial activity of RpCTL was dose-dependent. The recombinant RpCTL protein (200 μg/ml) had a strong inhibitory effect on microbial growth, whereas 20 μg/ml RpCTL had only a weak inhibitory effect. In an antimicrobial activity test, RpCTL inhibited the proliferation of pathogenic bacteria in vitro, thus exerting an antibacterial effect. rCFLec-1 is a recombinant CTL protein of *Chlamys farreri* that has a significant inhibitory effect on *Micrococcus luteus*, a Gram-positive bacterium, but a relatively weak bacteriostatic effect on *E. coli*, a Gram-negative bacterium [56]. Several studies of shrimp CTLs have also reported their inhibitory activity against bacteria [57]. In our study, the inhibition of *E. coli*, *V. anguillarum*, and *S. aureus* by RpCTL was stronger than its inhibition of *B. subtilis*. It has been reported that a number of CTLs have significant antibacterial activity. For example, several studies of *Eriocheir sinensis* have shown that its CTL has different and significant inhibitory effects on the growth of various microorganisms [58–60]. In the present study, the inhibition of microbial activity by RpCTL was dose-dependent. The results of a microbiological activity assay indicated that RpCTL inhibits the proliferation of pathogens in vitro.

C-type lectins and C3 molecules have a conserved thioester bond. In the immune response, they covalently bind to the surfaces of exogenous microorganisms through this thioester bond, triggering a series of downstream immune reactions, such as the activation of the terminal complement pathway, the induction of phagocytosis, etc. [61,62]. To investigate the immunoprotective effect of RpCTL in *R. philippinarum*, we injected clams with RpCTL and *V. anguillarum* and observed their survival rates. The survival rate of clams infected with *V. anguillarum* decreased sharply in the RpCTL-untreated group, whereas the survival rate of infected clams was higher in the RpCTL-treated group than in the PBS-treated group, indicating that RpCTL plays an important role in the immune defense of *R. philippinarum*.

In conclusion, a new RpCTL was cloned from *R. philippinarum* with RACE. *RpCTL* mRNA was mainly expressed in the siphon, gill, and hepatopancreas, with low expression in the mantle, foot, and adductor muscle, and its expression was significantly affected by LPS stimulation. A recombinant RpCTL protein was expressed in an *E. coli* expression system was investigated in this study. The recombinant RpCTL protein inhibited infections with pathogenic bacteria by killing or inhibiting the growth of both Gram-positive and Gram-negative bacteria. The results of this study indicate that RpCTL is an important immune-related protein involved in the immune defense responses of *R. philippinarum* to the LPS of Gram-negative bacteria. RpCTL is probably involved in pattern recognition and the immune elimination of important pathogen molecules from the clam.

Acknowledgments

We are grateful to the editor and anonymous reviewers for their helpful comments and constructive suggestions. Thanks given to Md Golam Rbbani for helping English grammar correction in the paper. This research was funded by the Cultivation Plan for Youth Agricultural Science and Technology Innovative Talents of Liaoning Province (2014004), the Modern Agro-industry Technology Research System (CARS-49), the Scientific Research project of Liaoning Education Department (QL201703), and Dalian high level talent innovation support program (Dalian Youth Science and Technology Star Project Support Program) (2016RQ065).

References

[1] T. Aoki, T. Takano, M.D. Santos, et al., Molecular innate immunity in teleost fish? Review and future perspectives, Fisheries for Global Welfare and Environment, 5th World Fisheries Congress, 2008, pp. 263–276.
[2] M. Marques, M.A. Barracco, Lectins, as non-self-recognition factors, in crustaceans, Aquaculture 191 (1) (2000) 23–44.
[3] S. Akira, S. Uematsu, O. Takeuchi, Pathogen recognition and innate immunity, Cell 124 (4) (2006) 783–801.
[4] Y.C. Liu, F.H. Li, B. Dong, et al., Molecular cloning, characterization and expression analysis of a putative C-type lectin (Fclectin) gene in Chinese shrimp *Fenneropenaeus chinensis*, Mol. Immunol. 44 (4) (2007) 598–607.
[5] S.V. Nair, M. Burandt, A. Hutchinson, et al., A C-type lectin from the tunicate, Styela plicata, that modulates cellular activity, Comp. Biochem. Physiol. C Toxicol. Pharmacol. 129 (1) (2001) 11–24.
[6] H. Wang, L. Song, C. Li, et al., Cloning and characterization of a novel C-type lectin from Zhikong scallop *Chlamys farreri*, Mol. Immunol. 44 (5) (2007) 722–731.
[7] X.Q. Yu, M.R. Kanost, A family of C-type lectins in *Manduca sexta*, Adv. Exp. Med. Biol. 484 (484) (2001) 191.
[8] Y.K. Jin, M. Adhya, S.K. Cho, et al., Characterization, tissue expression, and immunohistochemical localization of MCL3, a C-type lectin produced by *Perkinsus olseni* -infected Manila clams (*Ruditapes philippinarum*), Fish Shellfish Immunol. 25 (5) (2008) 598–603.
[9] N. Wang, I. Whang, J. Lee, A novel C-type lectin from abalone, *Haliotis discus discus*, agglutinates *Vibrio alginolyticus*, Dev. Comp. Immunol. 32 (9) (2008) 1034–1040.
[10] X. Jing, E.P. Espinosa, M. Perrigault, et al., Identification, molecular characterization and expression analysis of a mucosal C-type lectin in the eastern oyster, *Crassostrea virginica*, Fish Shellfish Immunol. 30 (3) (2011) 851–858.
[11] H. Zhang, X. Song, L. Wang, et al., AiCTL-6, a novel C-type lectin from bay scallop *Argopecten irradians*, with a long C-type lectin-like domain, Fish Shellfish Immunol. 30 (1) (2011) 17.
[12] H. Wang, L. Song, C. Li, et al., Cloning and characterization of a novel C-type lectin from Zhikong scallop *Chlamys farreri*, Mol. Immunol. 44 (5) (2007) 722–731.
[13] P. Zheng, H. Wang, J. Zhao, et al., A lectin (CfLec-2) aggregating Staphylococcus haemolyticus from scallop *Chlamys farreri*, Fish Shellfish Immunol. 24 (3) (2008) 286–293.
[14] H. Zhang, H. Wang, L. Wang, et al., A novel C-type lectin (Cflec-3) from *Chlamys farreri* with three carbohydrate-recognition domains, Fish Shellfish Immunol. 26 (5) (2009) 707–715.
[15] J.C. Jr, R. Medzhitov, Innate immune recognition, Annu. Rev. Immunol. 20 (1) (2002) 197–216.
[16] R. Medzhitov, C.A. Janeway, Decoding the patterns of self and nonself by the innate immune system, Science 296 (5566) (2002) 298–300.
[17] S. Akira, S. Uematsu, O. Takeuchi, Pathogen recognition and innate immunity, Cell 124 (4) (2006) 783–801.
[18] T.H. Ma, J.A. Benzie, J.G. He, et al., PmLT, a C-type lectin specific to hepatopancreas is involved in the innate defense of the shrimp *Penaeus monodon*, J. Invertebr. Pathol. 99 (3) (2008) 332–341.
[19] A.N. Zelensky, J.E. Gready, The C-type lectin-like domain superfamily, FEBS J. 272 (24) (2005) 6179–6217.
[20] X.Q. Yu, M.R. Kanost, Immulectin-2, a pattern recognition receptor that stimulates hemocyte encapsulation and melanization in the tobacco hornworm, *Manduca sexta*, Dev. Comp. Immunol. 28 (9) (2004) 891–900.
[21] A. K Drickamer, M.E. Taylor, Biology of animal lectins, Annu. Rev. Cell Biol. 9 (1) (1993) 237–264.
[22] R.B. Dodd, K. Drickamer, Lectin-like proteins in model organisms: implications for evolution of carbohydrate-binding activity, Glycobiology 11 (5) (2001) 71R-9R.
[23] X.Q. Yu, M.R. Kanost, Immulectin-2, a pattern recognition receptor that stimulates hemocyte encapsulation and melanization in the tobacco hornworm, *Manduca*

sexta, Dev. Comp. Immunol. 28 (9) (2004) 891–900.
[24] K. Drickamer, Evolution of Ca(2+)-dependent animal lectins, Prog. Nucleic Acid Res. Mol. Biol. 45 (1993) 207.
[25] W.I. Weis, R. Kahn, R. Fourme, et al., Structure of the calcium-dependent lectin domain from a rat mannose-binding protein determined by MAD phasing, Science 254 (5038) (1991) 1608–1615.
[26] FAO. Global Production Statistics 1950-2014: *Ruditapes philippinarum* [Internet]. http://www.fao.org/fishery/species/3543/en Accessed 14 December 2016.
[27] G.F. Zhang, X.W. Yan, Clam Aquaculture, Science Press, Beijing, China, 2010 (in Chinese).
[28] L.Q. Zhao, X.W. Yan, Huo, Feng Yang, Guofan Zhang, Divergent selection for shell length in the Manila clam *Ruditapes philippinarum*, J. World Aquacult. Soc. 43 (6) (2012) 878–884.
[29] C. Paillard, F.L. Roux, J.J. Borrego, Bacterial disease in marine bivalves, a review of recent studies: trends and evolution, Aquat. Living Resour. 17 (4) (2004) 477–498.
[30] T. Waki, J. Shimokawa, S. Watanabe, et al., Experimental challenges of wild Manila clams with Perkinsus species isolated from naturally infected wild Manila clams, J. Invertebr. Pathol. 111 (1) (2012) 50–55.
[31] H. Nie, L. Jiang, Z. Huo, et al., Transcriptomic responses to low temperature stress in the Manila clam, *Ruditapes philippinarum*, Fish Shellfish Immunol. 55 (2016) 358–366.
[32] H. Lis, N. Sharon, Lectins: carbohydrate-specific proteins that mediate cellular recognition, Chem. Rev. 98 (2) (1998) 637–674.
[33] Z.Y. Fang, L. Dan, X.J. Li, et al., A single CRD C-type lectin from *Eriocheir sinensis*, (EsLecB) with microbial-binding, antibacterial prophenoloxidase activation and hem-encapsulation activities[J], Fish Shellfish Immunol. 50 (2016) 175–190.
[34] X.K. Jin, W.W. Li, L. Cheng, et al., Two novel short C-type lectin from Chinese mitten crab, *Eriocheir sinensis*, are induced in response to LPS challenged, Fish Shellfish Immunol. 33 (5) (2012) 1149–1158.
[35] N. Saitou, M. Nei, The neighbor-joining method: a new method for reconstructing phylogenetic trees, Mol. Biol. Evol. 4 (4) (1987) 406.
[36] K.J. Livak, T.D. Schmittgen, Analysis of relative gene expression data using real-time quantitative PCR and the 2(-Delta Delta C(T)) method, Methods 25 (4) (2001) 402–408.
[37] G.R. Vasta, H. Ahmed, E.W. Odom, Structural and functional diversity of lectin repertoires in invertebrates, protochordates and ectothermic vertebrates, Curr. Opin. Struct. Biol. 14 (5) (2004) 617.
[38] A. K Drickamer, M.E. Taylor, Biology of animal lectins, Annu. Rev. Cell Biol. 9 (1) (1993) 237–264.
[39] R.B. Dodd, K. Drickamer, Lectin-like proteins in model organisms: implications for evolution of carbohydrate-binding activity, Glycobiology 11 (5) (2001) 71R-9R.
[40] A.N. Zelensky, J.E. Gready, The C-type lectin-like domain superfamily, FEBS J. 272 (24) (2005) 6179–6217.
[41] A.J. Day, The C-type carbohydrate recognition domain (CRD) superfamily, Biochem. Soc. Trans. 22 (1) (1994) 83–88.
[42] C.H. Li, J. Chen, Molecular cloning, characterization and expression analysis of a novel wap65-1 gene from *Plecoglossus altivelis*, Comp. Biochem. Physiol B Biochem. Mol. Biol. 44 (2) (2015) 603–610.
[43] J. Wei, D. Xu, J. Zhou, et al., Molecular cloning, characterization and expression analysis of a C-type lectin (Ec-CTL) in orange-spotted grouper, *Epinephelus coioides*, Fish Shellfish Immunol. 28 (1) (2010) 178–186.
[44] S. Yu, H. Yang, Y. Chai, et al., Molecular cloning and characterization of a C-type lectin in roughskin sculpin (*Trachidermus fasciatus*), Fish Shellfish Immunol. 34 (2) (2013) 582–592.
[45] H. Kondo, A.G. Yeu Tzeh, I. Hirono, et al., Identification of a novel C-type lectin gene in Japanese flounder, *Paralichthys olivaceus*, Fish Shellfish Immunol. 23 (5) (2007) 1089–1094.
[46] H. Zhang, P. Kong, L. Wang, et al., Cflec-5, a pattern recognition receptor in scallop *Chlamys farreri* agglutinating yeast Pichia pastoris, Fish Shellfish Immunol. 29 (1) (2010) 149–156.
[47] X. Song, H. Zhang, L. Wang, et al., A galectin with quadruple-domain from bay scallop *Argopecten irradians* is involved in innate immune response, Dev. Comp. Immunol. 35 (5) (2011) 592–602.
[48] S. Tasumi, G.R. Vasta, A galectin of unique domain organization from hemocytes of the Eastern oyster (*Crassostrea virginica*) is a receptor for the protistan parasite Perkinsus marinus, J. Immunol. 179 (5) (2007) 3086–3098.
[49] X.Y. Song, H. Zhang, J.M. Zhao, et al., An immune responsive multidomain galectin from bay scallop *Argopectens irradians*, Fish Shellfish Immunol. 28 (2) (2010) 326–332.
[50] P.F. Kong, H. Zhang, L.L. Wang, et al., AiC1qDC-1, a novel gC1q-domain-containing protein from bay scallop *Argopecten irradians* with fungi agglutinating activity, Dev. Comp. Immunol. 34 (8) (2010) 837–846.
[51] E.E. Prokhorova, N.V. Tsymbalenko, G.L. Ataev, Expression of genes encoding defense factors in the snail Planorbarius corneus (*Gastropoda, Pulmonata*) infested with trematodes, Parazitologiia 44 (4) (2010) 310.
[52] C. Mu, L. Chen, J. Zhao, et al., Molecular cloning and expression of a C-type lectin gene from *Venerupis philippinarum*, Mol. Biol. Rep. 41 (1) (2014) 139.
[53] X. Wei, J. Yang, X. Liu, et al., Identification and transcriptional analysis of two types of lectins (*SgCTL-1* and *SgGal-1*) from mollusk *Solen grandis*, Fish Shellfish Immunol. 33 (2) (2012) 204–212.
[54] Y.D. Sun, L.D. Fu, Y.P. Jia, X.J. Du, Q. Wang, Y.H. Wang, et al., A hepatopancreas-specific C-type lectin from the Chinese shrimp *Fenneropenaeus chinensis* exhibits antimicrobial activity, Mol. Immunol. 45 (2008) 348–361.
[55] X.W. Wang, W.T. Xu, X.W. Zhang, X.F. Zhao, X.Q. Yu, J.X. Wang, A C-type lectin is involved in the innate immune response of Chinese white shrimp, Fish Shellfish Immunol. 27 (2009) 556–562.
[56] H. Wang, L. Song, C. Li, J. Zhao, H. Zhang, D. Ni, et al., Cloning and characterization of a novel C-type lectin from Zhikong scallop *Chlamys farreri*, Mol. Immunol. 44 (2007) 722–731.
[57] Y.D. Sun, L.D. Fu, Y.P. Jia, X.J. Du, Q. Wang, Y.H. Wang, et al., A hepatopancreas-specific C-type lectin from the Chinese shrimp *Fenneropenaeus chinensis* exhibits antimicrobial activity, Mol. Immunol. 45 (2008) 348–361.
[58] X.K. Jin, S. Li, X.N. Guo, L. Cheng, M.H. Wu, S.J. Tan, et al., Two antibacterial C-type lectins from crustacean, *Eriocheir sinensis*, stimulated cellular encapsulation in vitro, Dev. Comp. Immunol. 41 (2013) 544–552.
[59] X.N. Guo, X.K. Jin, S. Li, A.Q. Yu, M.H. Wu, S.J. Tan, et al., A novel C-type lectin from *Eriocheir sinensis* functions as a pattern recognition receptor with anti-bacterial activity, Fish Shellfish Immunol. 35 (2013) 1554–1565.
[60] X.K. Jin, X.N. Guo, S. Li, et al., Association of a Hepatopancreas-Specific C-Type Lectin with the Antibacterial Response of *Eriocheir sinensis*, PLoS One 8 (10) (2013) e76132.
[61] J. Yang, L. Qiu, X. Wei, et al., An ancient C-type lectin inChlamys farreri(CfLec-2) that mediate pathogen recognition and cellular adhesion, Dev. Comp. Immunol. 34 (12) (2010) 1274–1282.
[62] S. Blandin, E.A. Levashina, Thiocstcr-containing proteins and insect immunity, Mol. Immunol. 40 (12) (2004) 364–374.